Tyrosine hydroxylase down-regulation after loss of Abelson helper integration site 1 (AHI1) promotes depression via the circadian clock pathway in mice

Received for publication, October 26, 2017, and in revised form, February 9, 2018 Published, Papers in Press, February 15, 2018, DOI 10.1074/jbc.RA117.000618

Dongkai Guo[‡], Shun Zhang[‡], Hongyang Sun[‡], Xingyun Xu[‡], Zongbing Hao[‡], Chenchen Mu[‡], Xingshun Xu[§¶], Guanghui Wang[‡1], and Haigang Ren[‡2]

From the [‡]Laboratory of Molecular Neuropathology, Jiangsu Key Laboratory of Neuropsychiatric Disorders and Department of Pharmacology, College of Pharmaceutical Sciences, Soochow University, Suzhou, Jiangsu 215123, China, the [§]Institute of Neuroscience, Soochow University, Suzhou City, Jiangsu 215123, China, and the [¶]Department of Neurology, Second Affiliated Hospital of Soochow University, Suzhou 215004, China

Edited by Xiao-Fan Wang

Abelson helper integration site 1 (AHI1) is associated with several neuropsychiatric and brain developmental disorders, such as schizophrenia, depression, autism, and Joubert syndrome. *Ahi1* deficiency in mice leads to behaviors typical of depression. However, the mechanisms by which AHI1 regulates behavior remain to be elucidated. Here, we found that down-regulation of expression of the rate-limiting enzyme in dopamine biosynthesis, tyrosine hydroxylase (TH), in the midbrains of *Ahi1*-knockout (KO) mice is responsible for *Ahi1*-deficiency–mediated depressive symptoms. We also found that Rev-Erbα, a *TH* transcriptional repressor and circadian regulator, is up-regulated in the *Ahi1*-KO mouse midbrains and *Ahi1*-knockdown Neuro-2a cells. Moreover, brain and muscle Arnt-like protein 1 (BMAL1), the *Rev-Erbα* transcriptional regulator, is also increased in the *Ahi1*-KO mouse midbrains and *Ahi1*-knockdown cells. Our results further revealed that AHI1 decreases BMAL1/Rev-Erbα expression by interacting with and repressing retinoic acid receptor–related orphan receptor α, a nuclear receptor and transcriptional regulator of circadian genes. Of note, *Bmal1* deficiency reversed the reduction in TH expression induced by *Ahi1* deficiency. Moreover, microinfusion of the Rev-Erbα inhibitor SR8278 into the ventral midbrain of *Ahi1*-KO mice significantly increased TH expression in the ventral tegmental area and improved their depressive symptoms. These findings provide a mechanistic explanation for a link between AHI1-related behaviors and the circadian clock pathway, indicating an involvement of circadian regulatory proteins in AHI1-regulated mood and behavior.

Abelson helper integration site 1 (AHI1)[3] is associated with mental disorders and neural development. Mutations in *AHI1* are identified as a frequent factor of an autosomal recessive Joubert syndrome that is characterized by abnormal neurodevelopment and mental disturbance (1–3). Moreover, many lines of evidence indicate the linkage between AHI1 and neuropsychiatric disorders, including schizophrenia (SCZ) (4–7), depression (8), and autism (9). In an animal model, *Ahi1* knockout (KO) mice exhibit typical depressive behaviors, sharing common neurological characters in human psychiatric disorders, accompanied by decreases of neurotransmitters such as dopamine (DA) and serotonin (5-HT) in various brain regions (10–12). These findings suggest that AHI1 plays an essential role in mood and mood-related behavior regulation. However, the molecular pathways involved in the regulation of AHI1-related depressive behavior are still largely unknown.

Monoamines, including neurotransmitters DA, 5-HT, and noradrenaline, are disturbed in subjects with mood disorders (13, 14). Especially, mesolimbic DA pathways are important for brain activities in emotion, including reward, motivation, and hedonic tone. DA dysfunction has been implicated in many mental disorders, including depression, SCZ, autism spectrum disorder, obsessive compulsive disorder, and attention deficit-hyperactivity disorder (15–17). A decreased DA function in midbrain is closely related to pathophysiology of depression, whereas increased DA activity is involved in mania (15, 17, 18).

Circadian rhythms have important roles in mood regulation. Polymorphisms in many clock genes are associated with various psychiatric disorders (19–21). Circadian gene products regulate daily oscillation of monoamine neurotransmitters, by

This work was supported by National Natural Sciences Foundation of China Grants 81761148024, 31330030, and 31471012; National Key Scientific R&D Program of China Grants 2016YFC1306000 and 2012CB947602; Suzhou Clinical Research Center of Neurological Disease Grant Szzx201503; and a Project Funded by the Priority Academic Program Development of Jiangsu Higher Education Institutions. The authors declare that they have no conflicts of interest with the contents of this article.

This article contains Figs. S1–S4.

[1] To whom correspondence may be addressed. Tel.: 86-512-65884845; Fax: 86-512-65884845; E-mail: wanggh@suda.edu.cn.

[2] To whom correspondence may be addressed. Tel.: 86-512-65884845; Fax: 86-512-65884845; E-mail: rhg@suda.edu.cn.

[3] The abbreviations used are: AHI1, Abelson helper integration site 1; 5-HT, serotonin; BMAL1, brain and muscle Arnt-like protein 1; CLOCK, locomotor output cycle kaput; DA, dopamine; KO, knockout; FST, forced swim test; MAOA and MAOB, monoamine oxidase A and B, respectively; RORα, retinoic acid receptor–related orphan receptor α; NURR1, nuclear receptor-related protein 1; TH, tyrosine hydroxylase; TST, suspension test; VMB, ventral midbrain; VTA, ventral tegmental area; AP, anteroposterior; ML, medial lateral; DV, dorsal ventral; SCZ, schizophrenia; RRE, REV-ERBs/RORE; RORE, retinoic acid receptor–related orphan nuclear receptor response element; NBRE, NGFI-B response element; DAB, diaminobenzidine; CT, circadian time; HEK293, human embryonic kidney 293; ANOVA, analysis of variance; qPCR, quantitative PCR.

controlling either their biosynthesis or metabolism (19, 20, 22). Tyrosine hydroxylase (TH), a rate-limiting enzyme for DA biosynthesis, is directly repressed by circadian nuclear receptor Rev-Erbα (23, 24). Rev-Erbα binds to RRE (REV-ERBs/retinoic acid receptor–related orphan nuclear receptor response element (RORE))/NBRE (NGFI-B response element) elements in the *TH* promoter to repress TH expression via competing with nuclear receptor–related protein 1 (NURR1), a major transcriptional factor of *TH* (23, 25). TH expression is also negatively regulated by circadian locomotor output cycle kaput (CLOCK) that is heterodimerized with brain and muscle Arnt-like protein 1 (BMAL1) (26–28). Clock components BMAL1, neuronal PAS domain protein 2 (NPAS2; a paralog of CLOCK), and PERIOD 2 (PER2) also participate in mood regulation by transcriptionally regulating the expression of monoamine oxidase A (MAOA), an enzyme that degrades DA and 5-HT (29).

Here, we demonstrate that AHI1 affects mood and behavior through circadian protein-mediated TH expression. AHI1 binds to RORα and represses BMAL1 expression, subsequently inhibits Rev-Erbα expression, and in turn up-regulates TH expression. Loss of AHI1 increases BMAL1 and Rev-Erbα levels and leads to TH expression inhibition.

Results

Decreased TH expression in Ahi1 KO mouse midbrains and Ahi1 knockdown cells

The previous studies demonstrated that *Ahi1* KO mice present depression-like behaviors with a significant decrease of DA and 5-HT levels in many brain regions (10, 11). Considering that there are no differences in behaviors and AHI1 expression between *Ahi1* heterozygous ($Ahi1^{+/-}$) and wildtype mice (10, 11), we used $Ahi1^{+/-}$ mice as controls and investigated the depressive behaviors of *Ahi1* KO mice. *Ahi1* KO mice showed a significant increase of immobility as compared with controls in tail suspension test (TST) and forced swim test (FST) (Fig. 1, *A* and *B*), indicating that *Ahi1* deficiency indeed leads to depression in mice. To identify how AHI1 affects production or release of DA and 5-HT, we measured mRNA levels of the key enzymes and transporters that are involved in production or release of DA and 5-HT in *Ahi1* KO mouse midbrains and the littermate controls, including 5-HT biosynthetic enzymes tryptophan hydroxylase 1 and 2 (TPH1 and TPH2), DA biosynthetic enzyme TH and DOPA decarboxylase (DDC), 5-HT and DA metabolic enzymes MAOA and MAOB, DA metabolic enzyme catechol-*O*-methyltransferase (COMT), 5-HT transporter (5-HTT), DA transporter (DAT), and vesicular monoamine transporter 2 (VMAT2). Interestingly, *TH* mRNA levels but not others were significantly decreased in *Ahi1* KO mouse midbrains (Fig. 1*C*). Consistently, TH protein levels but not other detected proteins were decreased in *Ahi1* KO mouse midbrains (Fig. 1*D*). Interestingly, stereological analysis revealed that there is no difference of TH-positive neuron numbers in the ventral tegmental area (VTA) between *Ahi1* KO mice and the littermate controls using diaminobenzidine (DAB) staining (Fig. 1, *E* and *F*). However, immunofluorescence staining showed that the TH fluorescence intensity was significantly decreased in VTA of *Ahi1* KO mice compared with the littermate controls (Fig. 1, *G* and *H*). These data suggest that *Ahi1* KO mice have lower TH protein expression levels but no changes in the cell numbers of TH neurons.

Next, we verified the regulation of TH by AHI1 in cultured cells. In Neuro-2a (N2a) cells, knockdown of *Ahi1* by two targeted siRNAs significantly decreased both *TH* mRNA and TH protein levels (Fig. 1, *I* and *J*). Meanwhile, overexpression of exogenous EGFP-AHI1 markedly increased TH protein levels (Fig. S1*A*). To further identify whether AHI1 regulates *TH* promoter activity, we cloned a 2-kb promoter fragment of murine *TH* gene and inserted it into a luciferase reporter vector. Overexpression of EGFP-AHI1 in cells dramatically increased *TH* promoter-driven luciferase reporter activity (Fig. S1*B*).

Many studies indicated that expression of TH is a time-of-day circadian oscillating pattern, and its expression is lowered at daytime and raised at night in mouse brain (23, 28, 30). Therefore, we tested whether AHI1 affects TH expression at different times of the day. As shown in Fig. 1*K*, TH protein levels are higher at subjective dawn (circadian time 00, CT00) than at subjective dusk (CT12) in both $Ahi1^{+/-}$ and $Ahi1^{-/-}$ mouse midbrains. Moreover, TH protein levels are significantly lower in *Ahi1* KO mice midbrain than littermate controls at both CT00 and CT12 (Fig. 1, *K* and *L*). Taken together, our results suggested that *Ahi1* KO mice exhibit depression-like behaviors, at least in part, by decreasing TH transcriptional expression.

Increased Rev-Erbα expression in Ahi1 KO mouse midbrains and Ahi1 knockdown cells

NURR1 is a major transcriptional factor of *TH*, and the circadian nuclear receptor Rev-Erbα represses *TH* transcription via competing with NURR1 to bind to RRE/NBRE elements of the *TH* promoter (23, 25). Therefore, we measured whether AHI1 has an effect on expression of NURR1 or Rev-Erbα. In *Ahi1* KO mouse midbrains, Rev-Erbα protein levels were dramatically increased compared with the littermate controls; however, NURR1 protein levels kept unchanged (Fig. 2, *A* and *B*). Real-time qPCR analysis showed that *Rev-Erbα* but not *Nurr1* mRNA levels were elevated in *Ahi1* KO mouse midbrains (Fig. 2*C*). In cultured N2a cells, knockdown of *Ahi1* using siRNAs markedly increased Rev-Erbα protein as well as *Rev-Erbα* mRNA levels but did not affect NURR1 protein and mRNA levels (Fig. 2, *D* and *E*). We next identified the correlation between the decrease of TH and increase of Rev-Erbα expression caused by AHI1 deficiency. Knockdown of *Rev-erα* increases TH protein levels in cells (Fig. S2), consistent with a study by other investigators (23). We next cloned a mutant *TH* promoter that lacks a Rev-Erbα–binding site and investigated the effect of AHI1 on its activity (Fig. 2*F*). Interestingly, EGFP-AHI1 lost the ability to influence the mutant *TH* promoter activity (Fig. 2*G*). These results suggest that AHI1-mediated TH expression is dependent on negatively regulating Rev-Erbα but not NURR1 expression. In contrast to the TH circadian pattern (Fig. 1, *K* and *L*), Rev-Erbα protein levels are lower at CT00 than at CT12, and it is increased in *Ahi1* KO mouse midbrain compared with littermate controls at both CT00 and CT12 (Fig. 2, *H* and *I*).

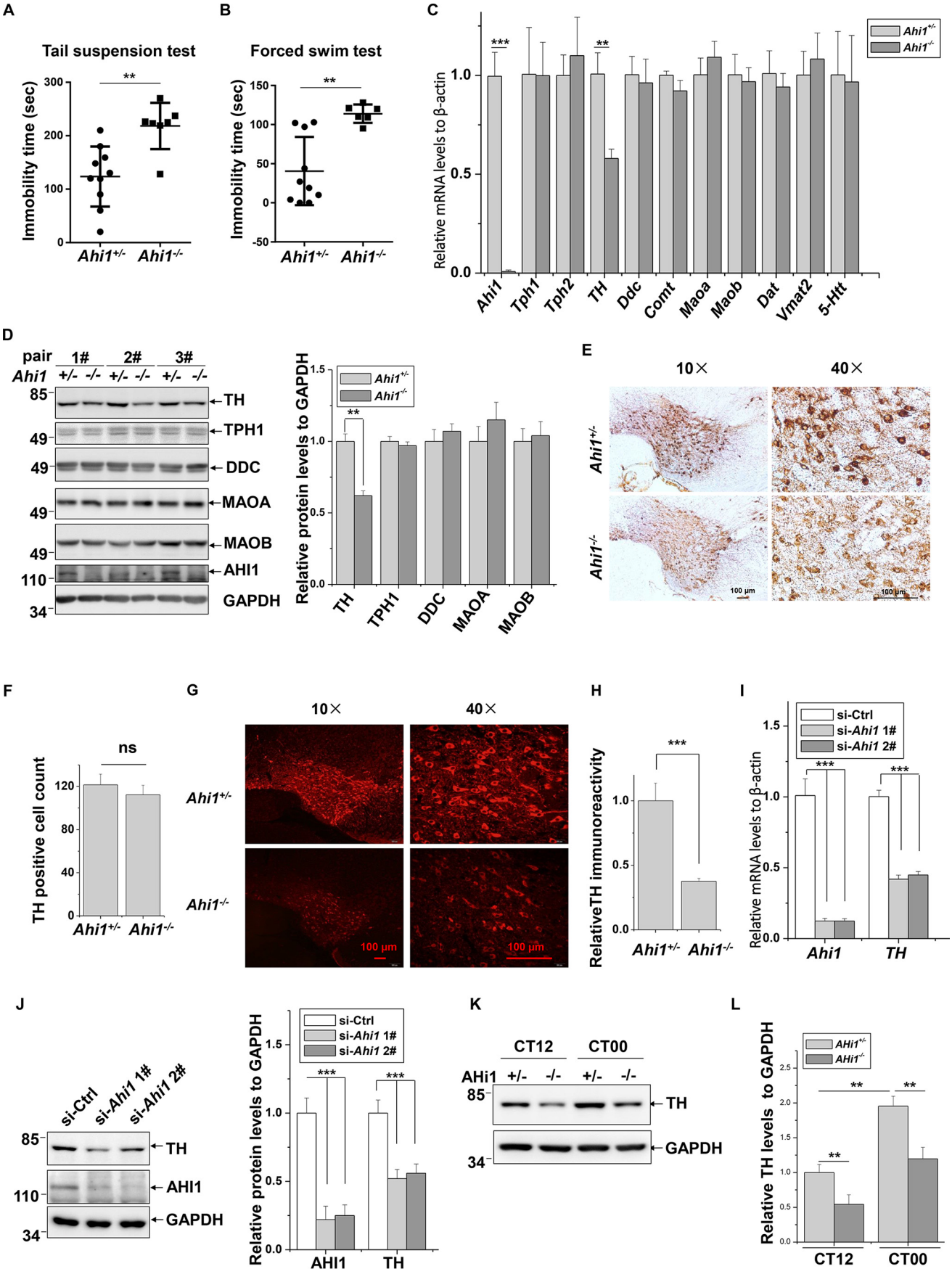
A
Tail suspension test
Immobility time (sec)
Ahi1+/-
Ahi1-/-
B
Forced swim test
Immobility time (sec)
C
Relative mRNA levels to β-actin
Ahi1
Tph1
Tph2
TH
Ddc
Comt
Maoa
Maob
Dat
Vmat2
5-Htt
D
pair
Ahi1
TH
TPH1
DDC
MAOA
MAOB
AHI1
GAPDH
Relative protein levels to GAPDH
E
10×
40×
100 μm
F
TH positive cell count
ns
G
10×
40×
100 μm
H
RelativeTH immunoreactivity
I
si-Ctrl
si-Ahi1 1#
si-Ahi1 2#
Relative mRNA levels to β-actin
J
si-Ctrl
si-Ahi1 1#
si-Ahi1 2#
K
CT12
CT00
L
Relative TH levels to GAPDH

Induction of Rev-Erbα expression by Ahi1 deficiency is BMAL1-dependent

BMAL1/CLOCK binds to the E-box element of the *Rev-Erbα* promoter to activate its transcription (31, 32). We therefore constructed two luciferase reporter vectors, a fragment of promoter in the *Rev-Erbα* gene (−1482/+502) (WT-Luc) and its deletion mutant (ΔCACATG (+24/+29)) (mutant-Luc), which lacks the BMAL1/CLOCK-binding site (Fig. 3*A*), to identify whether BMAL1 is involved in the regulation of Rev-Erbα by AHI1. Overexpression of EGFP-AHI1 repressed both basal and BMAL1/CLOCK-induced activities of the *Rev-Erbα* promoter (Fig. 3*A*). However, AHI1 did not affect activity of the mutant *Rev-Erbα* promoter (Fig. 3*A*). As the BMAL1/CLOCK-binding site in the *Rev-Erbα* promoter is involved in AHI1-regulated *Rev-Erbα* transcription, we examined whether BMAL1 and CLOCK are regulated by AHI1. In *Ahi1* knockdown cells, BMAL1 but not CLOCK protein levels were increased (Fig. 3*B*). Similar to results from *in vitro* assays, BMAL1 but not CLOCK protein levels were increased in *Ahi1* KO mouse midbrains (Fig. 3*C*). Moreover, *Bmal1* but not *Clock* mRNA levels were also increased in *Ahi1* knockdown cells (Fig. 3*D*), suggesting that AHI1 may transcriptionally regulate BMAL1 expression. Other clock genes, such as *Periods* (*Per1*, *Per2*, and *Per3*) and *Crytochromes* (*Cry1* and *Cry2*), are also transcriptionally controlled by BMAL1 (33). We therefore examined *Pers and Crys* mRNA levels and found that *Pers* and *Crys* genes were also up-regulated in *Ahi1* KO mouse midbrains (Fig. S4). *BMAL1* transcription is activated by transcriptional factor RORα (34). We next performed immunoprecipitation assays to examine the interactions between AHI1 and RORα. FLAG-RORα was co-precipitated when EGFP-AHI1 but not EGFP was precipitated using anti-GFP antibodies (Fig. 3*E*). We also performed immunocytochemistry staining to detect the distribution of AHI1 and RORα. Although EGFP-AHI1 was mainly distributed in cytoplasm, it partly localized in the nucleus and co-localized with FALG-RORα (Fig. 3*F*). Next, we examined whether AHI1 influences *Bmal1* promoter activity through RORα. The schematic diagrams of *Bmal1* promoter luciferase reporter and its deletion mutant lacking two ROREs that are responsible for RORα binding are shown (Fig. 3*G*). EGFP-AHI1 significantly repressed basal activity and RORα-induced activity of the *Bmal1* promoter (Fig. 3*G*). However, EGFP-AHI1 did not repress activity of the mutant *Bmal1* promoter (Fig. 3*G*). These data suggest that AHI1 interacts with RORα to repress *Bmal1* transcription.

Regulation of TH by AHI1 is BMAL1-dependent

We have shown that AHI1 deficiency reduces TH expression and up-regulates Rev-Erbα levels and that overexpression of AHI1 decreases BMAL1 expression. We wondered whether the regulation of TH expression by AHI1 is mediated by BMAL1-regulated Rev-Erbα expression. In *Bmal1* knockdown cells, increase of TH and decrease of Rev-Erbα protein levels were observed (Fig. 4*A*). Moreover, *TH* and *Rev-Erbα* mRNA levels were altered simultaneously in *Bmal1* knockdown cells (Fig. 4*B*). We next examined the effects of BMAL1/CLOCK on *TH* promoter activity. BMAL1/CLOCK dramatically repressed *TH* promoter activity, and BMAL1/CLOCK had no significant effect on the mutant *TH* promoter lacking the Rev-Erbα–binding site, indicated by reporter gene assays (Fig. S3). Moreover, increase of Rev-Erbα and decrease of TH protein levels induced by *Ahi1* knockdown were completely eliminated by BMAL1 deficiency (Fig. 4*C*), further suggesting that AHI1-induced TH expression is mediated by the BMAL1/CLOCK/Rev-Erbα circadian pathway.

Rev-Erbα inhibition prevents TH reduction and improves depressive behaviors of Ahi1 KO mice

As Rev-Erbα up-regulation contributes to the decreased TH expression induced by AHI1 deficiency, we wondered whether Rev-Erbα inhibition has impacts on TH expression and behavior of *Ahi1* KO mice. We microinfused SR8278, a Rev-Erbα inhibitor, into the VMB of *Ahi1* KO mice or control mice to inhibit midbrain Rev-Erbα activity. We examined TH expressions in VTA after SR8278 microinfusion. Although SR8278 did not significantly affect TH levels in control mice, TH levels were dramatically increased in VTA in *Ahi1* KO mice after SR8278 administration (Fig. 5, *A* and *B*). In addition, SR8278 administration significantly improved the performance of *Ahil* KO mice in TST but did not significantly affect the control mice (Fig. 5*C*).

Discussion

In the present study, we revealed that AHI1 regulates *TH* transcriptional expression through the circadian RORα/BMAL1/Rev-Erbα pathway, to participate in mood and behavior regulation. TH is a rate-limiting enzyme of biosynthesis of catecholamines, such as DA, noradrenaline, and epinephrine, by converting tyrosine to L-3,4-dihydroxyphenylalanine (L-DOPA) (35). It has been reported that the *TH* gene is associated with depressive disorder or bipolar disorder (36, 37). Our study demonstrates that AHI1-regulated TH expression may con-

Figure 1. Decreased TH expression in *Ahi1* KO mouse midbrains and *Ahi1* knockdown cells. *A*, immobility time in TST was measured in control mice ($n = 10$) and *Ahi1* KO mice ($n = 7$). **, $p < 0.01$. *B*, immobility time in FST was measured in control mice ($n = 10$) and *Ahi1* KO mice ($n = 6$). **, $p < 0.01$. *C*, relative mRNA levels of the indicated genes of *Ahi1* KO mouse midbrains and littermate controls were performed by real-time qPCR. **, $p < 0.01$ ($n = 5$). *D*, the indicated protein abundance of *Ahi1* KO mouse midbrains and the littermate controls was performed by Western blot analysis. The levels of the indicated proteins relative to GAPDH are shown on the *right*. **, $p < 0.01$ ($n = 3$). *E*, representative images of TH-DAB staining in VTA of *Ahi1* KO mice and the littermate controls are shown at AP −3.5 mm. *F*, quantification of the TH-positive cells from (*E*) was shown. *ns*, no statistical significance ($n = 3$). *G*, representative images of TH-fluorescence staining in VTA of *Ahi1* KO mice and the littermate controls are shown at AP −3.5 mm. *H*, intensity of TH immunofluorescence signals in *G* was analyzed. ***, $p < 0.001$ ($n = 3$). *I*, N2a cells were transfected with the indicated siRNAs. Seventy-two h after transfection, real-time qPCR was performed. *, $p < 0.001$ ($n = 3$). *J*, N2a cells were transfected with indicated siRNAs. Seventy-two h after transfection, the total cell lysates were subjected to immunoblot analysis. The intensities of AHI1 or TH relative to GAPDH (*right*) were analyzed. ***, $p < 0.001$ ($n = 3$). *K*, TH protein abundance of *Ahi1* KO mouse midbrain and littermate controls at CT12 and CT00 by Western blot analysis. *L*, the relative ratios of TH to GAPDH in *I* were analyzed from density analysis by one-way ANOVA. Data are presented as means ± S.E. (*error bars*). **, $p < 0.01$ ($n = 3$).

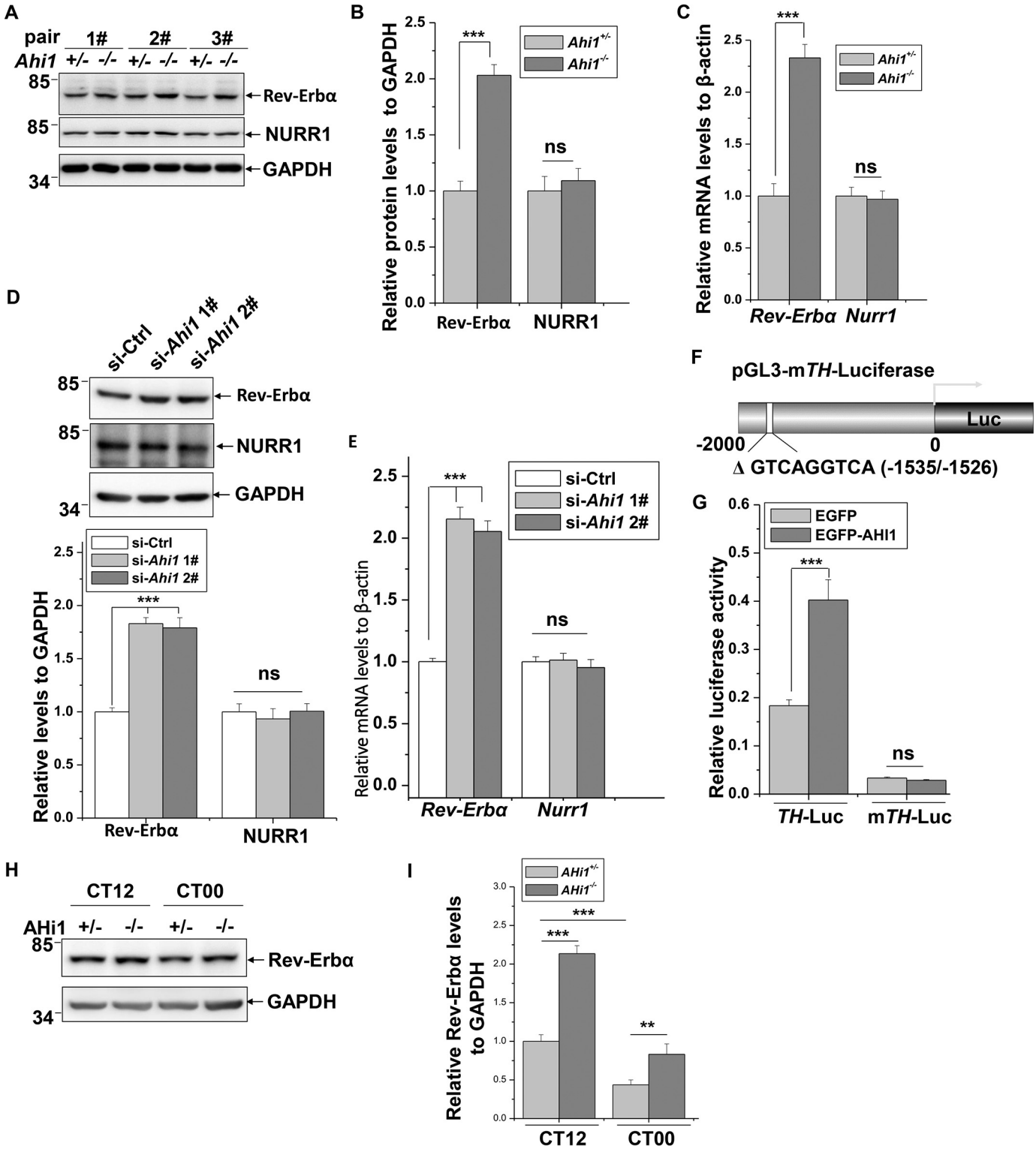

Figure 2. Increased Rev-Erbα expression in *Ahi1* KO mouse midbrains and *Ahi1* knockdown cells. *A*, the indicated protein abundance of *Ahi1* KO mouse midbrains and littermate controls was examined using immunoblot analysis ($n = 3$). *B*, the relative levels of the indicated proteins to GAPDH in *A* were analyzed. ***, $p < 0.001$; *ns*, no statistical significance ($n = 3$). *C*, relative mRNA levels of *Rev-Erbα* and *TH* of *Ahi1* KO mouse midbrains and littermate controls were examined using real-time qPCR. ***, $p < 0.001$; *ns*, no statistical significance ($n = 5$). *D*, N2a cells were transfected with the indicated siRNAs. Seventy-two h after transfection, the cell lysates were subjected to immunoblot analysis. The relative levels of Rev-Erbα and NURR1 to GAPDH (*bottom*) were analyzed. ***, $p < 0.001$; *ns*, no statistical significance ($n = 3$). *E*, N2a cells were transfected with the indicated siRNAs. Seventy-two h after transfection, real-time qPCR was performed. ***, $p < 0.001$; *ns*, no statistical significance ($n = 3$). *F*, schematic representation of mutant *TH* (*mTH*) promoter that lacks the Rev-Erbα binding motif in PGL3-Basic vector. *G*, HEK293 cells were transfected with PGL3-*TH*-Luc or PGL3-m*TH*-Luc along with EGFP or EGFP-AHI1, respectively. Forty-eight h after transfection, luciferase reporter assays were performed. ***, $p < 0.001$; *ns*, no statistical significance ($n = 3$). *H*, Rev-Erbα protein abundance of *Ahi1* KO mouse midbrain and littermate controls at CT12 and CT00 by Western blot analysis. *I*, the relative ratios of Rev-Erbα to GAPDH in *H* were analyzed from density analysis by one-way ANOVA. Data are presented as means ± S.E. (*error bars*). ***, $p < 0.001$; **, $p < 0.01$ ($n = 3$).

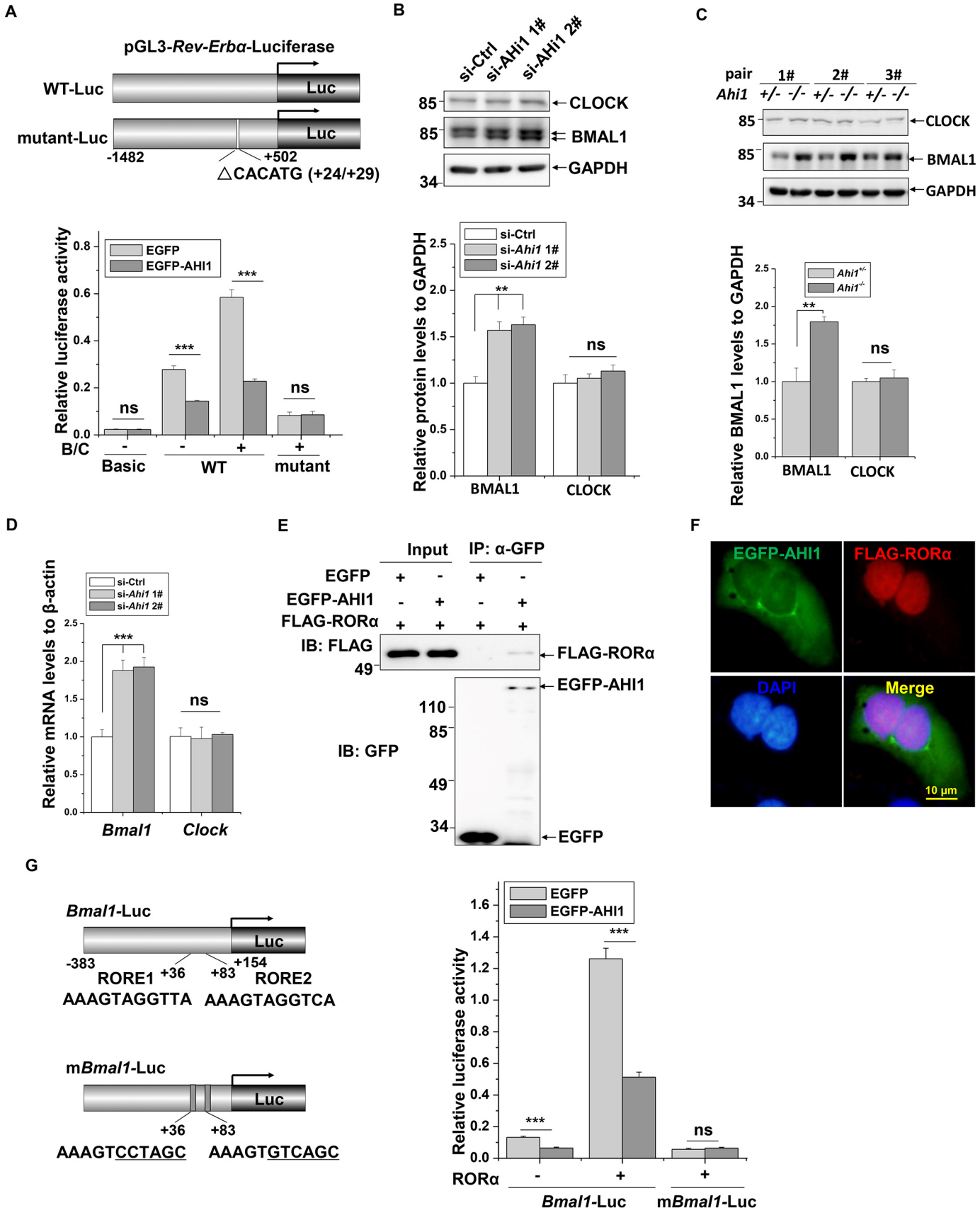
A
pGL3-Rev-Erbα-Luciferase
WT-Luc
Luc
mutant-Luc
Luc
-1482
+502
△CACATG (+24/+29)
Relative luciferase activity
EGFP
EGFP-AHI1
ns
***
***
ns
B/C
-
-
+
+
Basic
WT
mutant
B
si-Ctrl
si-AHi1 1#
si-AHi1 2#
85
CLOCK
85
BMAL1
34
GAPDH
Relative protein levels to GAPDH
si-Ctrl
si-Ahi1 1#
si-Ahi1 2#
**
ns
BMAL1
CLOCK
C
pair
1#
2#
3#
Ahi1
+/- -/- +/- -/- +/- -/-
85
CLOCK
85
BMAL1
34
GAPDH
Relative BMAL1 levels to GAPDH
Ahi1+/-
Ahi1-/-
**
ns
BMAL1
CLOCK
D
Relative mRNA levels to β-actin
si-Ctrl
si-Ahi1 1#
si-Ahi1 2#
***
ns
Bmal1
Clock
E
Input
IP: α-GFP
EGFP
+
-
+
-
EGFP-AHI1
-
+
-
+
FLAG-RORα
+
+
+
+
IB: FLAG
49
FLAG-RORα
EGFP-AHI1
110
85
IB: GFP
49
34
EGFP
F
EGFP-AHI1
FLAG-RORα
DAPI
Merge
10 μm
G
Bmal1-Luc
Luc
-383
+154
RORE1
+36
+83
RORE2
AAAGTAGGTTA
AAAGTAGGTCA
mBmal1-Luc
Luc
+36
+83
AAAGTCCTAGC
AAAGTGTCAGC
EGFP
EGFP-AHI1
Relative luciferase activity
***
***
ns
RORα
-
+
+
Bmal1-Luc
mBmal1-Luc

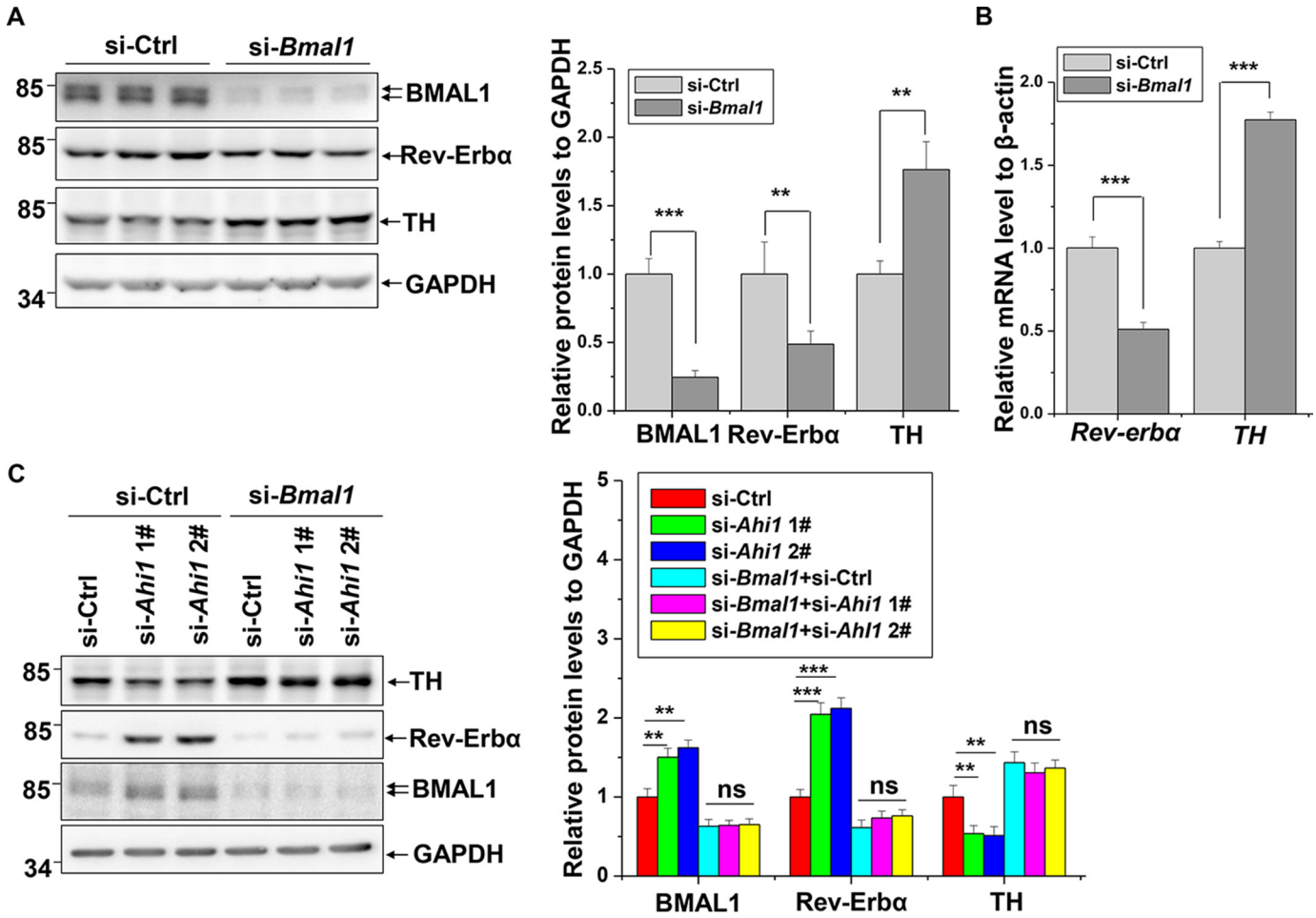

Figure 4. BMAL1-dependent regulation of TH by AHI1. *A*, N2a cells were transfected with si-Ctrl or si-*Bmal1*. Seventy-two h after transfection, the cell lysates were subjected to immunoblot analysis. The intensities of BMAL1, Rev-Erbα, or TH relative to GAPDH (*right*) were analyzed. ***, $p < 0.001$; **, $p < 0.01$ ($n = 3$). *B*, N2a cells were transfected with the indicated siRNAs. Seventy-two h after transfection, real-time qPCR was performed. ***, $p < 0.001$ ($n = 3$). *C*, N2a cells were transfected with the indicated siRNAs. Seventy-two h after transfection, the cell lysates were subjected to immunoblot analysis. The intensities of BMAL1, Rev-Erbα, or TH relative to GAPDH (*right*) were analyzed. ***, $p < 0.001$; **, $p < 0.01$; *, $p < 0.05$; *ns*, no statistical significance ($n = 3$). *Error bars*, S.E.

tribute to mood and behavior regulation. Decreased TH levels in the *Ahi1* KO mouse midbrain explain the decreased DA levels responsible for animal depressive behaviors.

AHI1 has comprehensive roles in mental regulation. *Ahi1* KO mice also show depressive phenotypes (10, 11). AHI1 is abundant in the hypothalamus and amygdale, the regions that are important for emotional regulation, and loss of AHI1 influences TrkB signaling involved in depression behaviors (11, 38). In our study, we further found that AHI1 deficiency induces decreases of TH levels in VTA. As DA in VTA is important for emotional regulation, our study suggests an involvement of DA in AHI1-deficiency–induced depressive behavior.

TH expression is activated by NURR1 or repressed by circadian clock protein Rev-Erbα through competing for binding to the NBRE motif in the *TH* promoter (23, 25). In our observation, AHI1 does not affect NURR1 expression, but AHI1 deficiency induces Rev-Erbα expression. In addition, *TH* promoter activity that lacks the NBRE motif cannot be regulated by AHI1, further suggesting that Rev-Erbα is involved in AHI1-regulated TH expression. It was reported that loss of AHI1 impairs TrkB

Figure 3. BMAL1-dependent induction of Rev-Erbα expression by *Ahi1* deficiency. *A*, schematic representation of wildtype (*WT-Luc*) and mutant *Rev-Erbα* promoters (*mutant-Luc*) that were constructed into PGL3-Basic vector. HEK293 cells were transfected with WT or mutant *Rev-Erbα*-Luc along with EGFP, EGFP-AHI1 or HA, HA-BMAL1/HA-CLOCK (B/C), respectively. Forty-eight h after transfection, a luciferase reporter assay was performed. ***, $p < 0.001$; *ns*, no statistical significance ($n = 3$). *B*, N2a cells were transfected with the indicated siRNAs. Seventy-two h after transfection, the cell lysates were subjected to immunoblot analysis. The intensities of BMAL1 and CLOCK relative to GAPDH (*bottom*) were analyzed. **, $p < 0.01$ ($n = 3$). *C*, the BMAL1 and CLOCK protein levels of *Ahi1* KO mouse midbrains and the littermate controls were examined using immunoblot analysis ($n = 3$). The intensity of BMAL1 relative to GAPDH (*bottom*) was analyzed. **, $p < 0.01$ ($n = 3$). *D*, N2a cells were transfected with the indicated siRNAs. Seventy-two h after transfection, real-time qPCR was performed. ***, $p < 0.001$; *ns*, no statistical significance ($n = 3$). *E*, HEK293 cells were transfected with FLAG-RORα along with EGFP or EGFP-AHI1. Forty-eight h after transfection, an immunoprecipitation assay was performed with anti-GFP antibodies. *F*, HEK293 cells were transfected with FLAG-RORα and EGFP-AHI1 (*green*). Forty-eight h after transfection, immunofluorescence was performed with anti-FLAG (*red*). The nuclei were stained with DAPI (*blue*). *G*, *left*, a *schematic representation* shows the WT and mutant *Bmal1* promoter luciferase reporter. *Right*, HEK293 cells were transfected with WT-Luc or mutant-Luc of *Bmal1* promoter along with EGFP, EGFP-AHI1 or FLAG, FLAG-RORα, respectively. Forty-eight h after transfection, a luciferase reporter assay was performed. ***, $p < 0.001$; *ns*, no statistical significance ($n = 3$). *Error bars*, S.E. *IP*, immunoprecipitation; *IB*, immunoblotting.

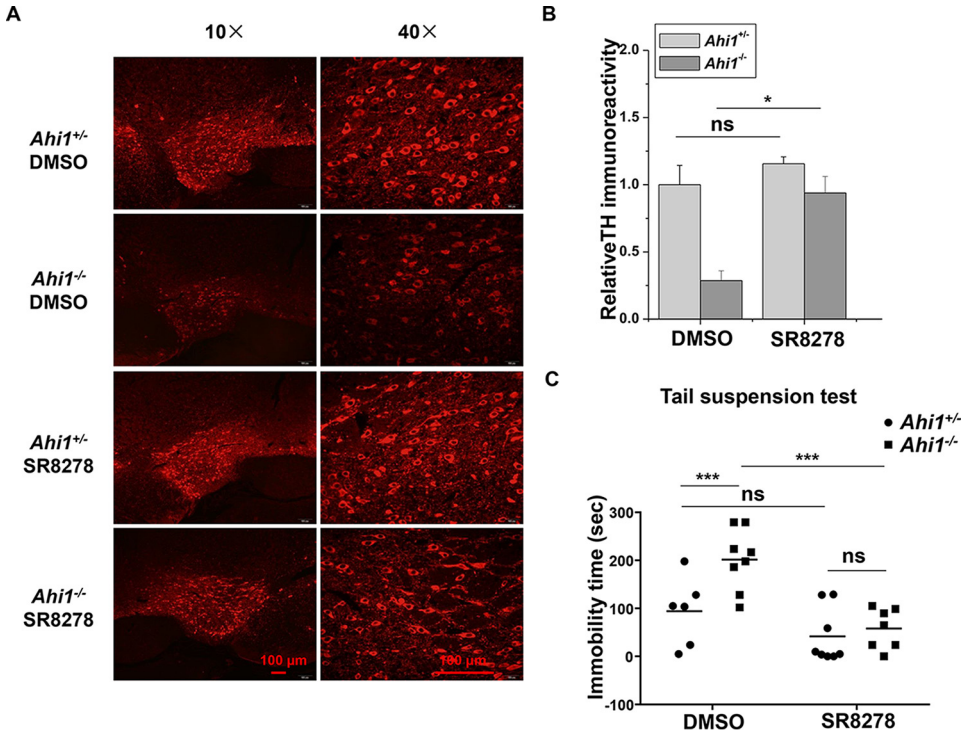

Figure 5. Restoration of TH levels and improvement of depressive behaviors of *Ahi1* KO mice by Rev-Erbα inhibition. *A–C*, SR8278 (16 μg/mouse) or an equal volume of DMSO was microinfused into the VMB of control mice or *Ahi1* KO mice. After 2 days, immunohistochemistry and TST were performed. *A*, fluorescence-TH staining of representative images in VTA were shown at AP −3.5 mm. *B*, intensity of TH immunofluorescence signals in *A* was analyzed. *, $p < 0.05$; *ns*, no statistical significance ($n = 3$). *C*, immobility time in TST was measured. Data are presented as means ± S.E. (*error bars*). **, $p < 0.01$; *ns*, no statistical significance ($n = 6–8$).

signaling (11). Interestingly, TrkB signaling activates TH expression through activating its promoter (39). In addition, TrkB activity is also regulated by the circadian clock pathway, showing that TrkB activity is higher at night and lower during the day (40). Whether AHI1-mediated circadian rhythm regulation influences TrkB signaling and whether TrkB participates in AHI1-mediated TH regulation remain to be evaluated.

The core circadian proteins CLOCK and BMAL1 form heterodimers to activate the transcription of several clock genes, such as *PERs*, *CRYs*, *RORα*, and *Rev-Erbα*. In turn, PERs and CRYs form complexes to repress the transcriptional activity of CLOCK/BMAL1. On the other hand, RORα and Rev-Erbα competitively bind to ROREs in the *BMAL1* promoter to activate or repress its transcription, respectively (33).

The association between circadian rhythms and mood regulation as well as behavior processes has been well-documented (41). Disruption of biological rhythms is considered as a hallmark for and one of the key contributors to several mental disorders, such as major depression (42, 43), bipolar disorder (44), and SCZ (45). Polymorphisms in several circadian genes have been identified to associate with mental disorders (20, 45, 46). Recently, many studies showed that circadian gene deficiency is associated with mood and behavior abnormalities in animals (47). For example, mice harboring the *Clock* mutant gene exhibit mania-like behavior with increased dopaminergic activity (26, 28), and *Per2* and *Bmal1* KO mice also display mania-like response (29, 48, 49). Interestingly, inhibition of Rev-Erbα by gene KO or inhibitor leads to emotional instability with mania-like behavior and hyperactivity by increasing TH protein levels and dopamine production (23). We also found that microinfusion of Rev-Erbα inhibitor SR8278 into the VMB of *Ahi1* KO mice significantly increases TH expression and reduces animal immobility time in TST. However, SR8278 only slightly increases TH expression and improves the control mouse performance in TST. The reason may be that Rev-Erbα is abundant in *Ahi1* KO mice as compared with control mice; thus, *Ahi1* KO mice are more sensitive to SR8278. This phenomenon is in accordance with the fact that SR8278 significantly reduces immobility time in Rev-Erbα high expression periods in a day rather than that in Rev-Erbα low expression periods (23). Thus, deficient Rev-Erbα activity in *Rev-Erbα* KO mice induces mania-like behavior, but increased Rev-Erbα levels in *Ahi1* KO mice result in depressive behavior; both show associations with alterations of TH and DA.

Although several E-box motifs are present in human, mouse, and rat *TH* promoters (23, 35), *TH* promoter activity cannot be activated by BMAL1/CLOCK in our observations. Conversely, BMAL1/CLOCK dramatically represses *TH* promoter activity, consistent with a reported study indicating that *TH* mRNA levels are augmented in *Clock* Δ19 mutant mice (26). BMAL1/CLOCK can bind to the E-box of *PER1* and activating transcription factor 5 (*ATF5*) promoters but not *TH* promoter by an electrophoretic mobility shift assay (30). These data suggest that BMAL1/CLOCK negatively regulate *TH* transcription by an indirect pathway. Considering that BMAL1/CLOCK activates *Rev-Erbα* transcription and Rev-Erbα directly represses TH expression (23, 31) and that *Rev-Erbα* and *TH* mRNA levels are attenuated and increased in *Clock* Δ19 mice (20, 26, 28), we propose that BMAL1/CLOCK inhibits TH expression via activating Rev-Erbα expression.

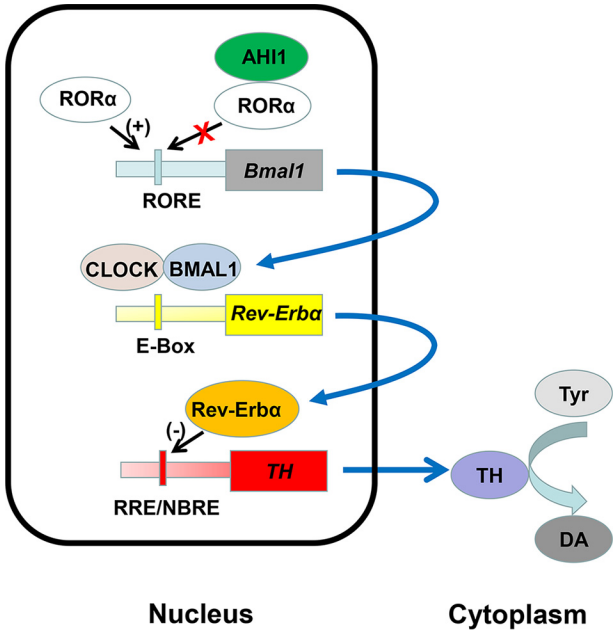

Figure 6. Schematic diagram of the pathway of TH expression and DA biosynthesis regulated by AHI1. AHI1 binds to the core circadian clock protein RORα and inhibits BMAL1 transcriptional expression. Decrease of BMAL1 results in down-regulation of Rev-Erbα expression and in turn up-regulates TH transcription and facilitates DA biosynthesis. Loss of AHI1 leads to increases of BMAL1/Rev-Erbα expressions, thereby repressing TH expression and DA biosynthesis, which contributes to animal depressive behaviors.

In conclusion, we identified that AHI1 binds to circadian protein RORα to negatively regulate BMAL1 and Rev-Erbα expressions, which eliminates Rev-Erbα–repressive effects and subsequently up-regulates TH expression, suggesting that AHI1 facilitates TH expression and DA biosynthesis through its regulating circadian clock pathway. Loss of AHI1 leads to an increase of Rev-Erbα that negatively regulates TH expression (Fig. 6). In conclusion, the present study demonstrates that the mood-related protein AHI1 links the molecular circadian clock pathway to regulate TH expression.

Experimental procedures

Plasmid constructs

pEGFP-C3-AHI1 was a gift from Joseph Gleeson (Addgene plasmid 30494) (50). HA-CLOCK, HA-BMAL1, FLAG-RORα, wildtype mouse *Bmal1*-luciferase (nucleotides −383 to +83), and mutant *Bmal1*-luciferase (mutation in RORE1 and RORE2) plasmids were kindly provided by Dr. Ying Xu (CAM-SU Genomic Resource Center at Soochow University). A 2.0-kb fragment of the *Rev-Erbα* promoter (nucleotides −1482 to +502) was amplified from a human genomic DNA library with the primers 5′-CGACGCGTGCTGCCTGTGGAGAAGGGCTT-3′ and 5′-CCCTCGAGGAAGCACCCTGCAGCAAGGTC-3′ and inserted into PGL3-Basic vector (Promega) at MluI/XhoI sites. Mutated *Rev-Erbα* promoter was constructed by deleting the BMAL1-binding E-box motif (CACATG (+24/+29)) (26, 27, 31) via site-directed mutagenesis with PGL3-*Rev-Erbα*-luciferase plasmid as template with primers 5′-GTACCTGCTCCAGTGCCG-3′ and 5′-ATCCCAGGGAGCGCCTCG-3′. A 2.0-kb fragment of the *TH* promoter (nucleotides −2001 to +0) was amplified from a mouse genomic DNA library with the primers 5′-GGGGTACCCAGCACCCTCTAAAGGAG-3′ and 5′-CCAAGCTTAGTGCAAGCTGGTGGTCC-3′ and inserted into PGL3-Basic vector at KpnI/HindIII sites. Mutated *TH* promoter that lacks the Rev-Erbα and NURR1 binding site (ΔGTCAGGTCA (−1535/−1526)) was generated by site-directed mutagenesis using PGL3-*TH*-luciferase plasmid as template with primers 5′-GCAGGGGAGGTTAGGGAGT-3′ and 5′-CCCCACAGTTCCTGTTCCAG-3′. The fidelities of all constructs were confirmed by sequencing.

Animals

Ahi1$^{+/-}$ and *Ahi1* homozygous (*Ahi1*$^{-/-}$) littermate mice were derived from *Ahi1*$^{+/-}$ and *Ahi1*$^{-/-}$ mice that were described previously (10). All animals were used according to the institutional guidelines for animal use and care, and all procedures were approved by the ethical committee of Soochow University. 8–10-week-old mice were housed in quarters under a 12-h light/12-h dark photoperiod (light on at 9:00 a.m.) and fed abundant food and water. Mice were sacrificed for collecting brain tissues at 2:00–4:00 pm except where specially indicated. CT00 was defined as lights on in the previous light/dark schedule when the mice were kept in constant darkness for 2 days.

Depression-like behaviors

The TST and FST were performed at 2:00–4:00 p.m. as described previously (10, 11). For TST, mice were hung in the 40-cm-high shelves by taping the tail (1–2 cm from tip). The immobility time was measured for 6 min. Mice were considered immobile when they gave up escaping or hung passively. For FST, mice were placed into a transparent beaker (16-cm diameter, 23-cm height) containing water (21–25 °C) at a depth of 15 cm. After a habituation period of 2 min, immobile time was measured within 4 min. Mice were considered as immobile when they floated or had slight limb movements.

Immunofluorescence and immunohistochemistry

Immunostaining was carried out as described previously (51). Mice were perfused with saline, followed by PBS (pH 7.4) containing 4% paraformaldehyde. Brains were removed and post-fixed in 4% paraformaldehyde overnight at 4 °C and then dehydrated with 30% sucrose for 2 days at 4 °C. After dehydration, the brain was cut into 30-μm-thick coronal sections including the VTA with freezing microtome (CM1900, Leica). Slices were incubated with anti-TH (AB152, Millipore) antibodies for 4 h. For immunofluorescence, slices were stained with rhodamine (red)-conjugated secondary antibody (Invitrogen) for 2 h. Finally, the slices were observed with an inverted system microscope Ti2-E (Nikon, Japan). TH immunofluorescence signals were also quantified by ImageJ software (National Institutes of Health). For immunohistochemistry, slices were incubated with anti-TH antibodies for 4 h, followed by the DAB staining using a non-biotin detection system (GTVision III Anti-Mouse/Rabbit-HRP; Gene Tech), and then slices were observed with an inverted system microscope Ti2-E.

Stereology and image analysis

To determine cell numbers and intensity of TH-immunoreactive neurons in the VTA, an unbiased stereological method

was performed according to the optical fractionator principle (52). Briefly, every fifth section (120-μm interval) was selected from each mouse and processed for immunostainings for TH using DAB staining. All images were acquired under the same conditions. The numbers of TH-immunoreactive neurons in the VTA were counted after outlining cell bodies and processes using ImageJ software.

Drug application

Mice were anesthetized by intraperitoneal injection of 4% chloral hydrate. Mice were placed prone, and heads were mounted in a stereotaxic apparatus (RWD Life Science Co, Shenzhen, China) by hooking incisors and inserting the ear stick into external auditory canal. Mouse skulls were exposed by cutting the scalp and corroding the meninges with H_2O_2. Bregma's location was set to the following: AP 0.0 mm, ML 0.0 mm, DV 0.0 mm. SR8278 was dissolved in DMSO to a concentration of 32 μg/μl and loaded into a 2.5-μl Hamilton syringe, which was fixed on a stereotaxic apparatus. SR8278 was infused into the VMB (AP $-$3.5 mm, ML $\pm$1.2 mm, DV $-$4.5 mm) (16 μg/mouse; a dose was performed according to the previous study (23)) at a rate of 0.1 μl/min. After injection, the injector needle was slowly pulled out at a uniform speed in 2 min to avoid bleeding. The mouse scalp was sutured, and mice were placed in a warm environment until they woke up naturally. TST and immunohistochemistry were executed 2 days after microinfusion.

Cell culture and plasmid transfection

Mouse neuroblastoma N2a cells and human embryonic kidney 293 (HEK293) cells were grown in Dulbecco's modified Eagle's medium (Gibco) containing 10% fetal bovine serum (Gibco) with streptomycin (100 μg/ml) and penicillin (100 units/ml) (Gibco). For plasmid transfection, cells were transfected with plasmids using Lipofectamine 2000 transfection reagent (Invitrogen) according to the manufacturer's instructions.

Immunocytochemistry

HEK293 cells transfected with EGFP-AHI1 and FLAG-RORα were washed with PBS twice and fixed with 4% paraformaldehyde for 10 min at room temperature. After treatment with 0.25% Triton X-100 for 15 min, the cells were incubated with 4% fetal bovine serum and anti-FLAG antibody (F3165, Sigma) in PBS overnight at 4 °C. Next, the cells were incubated with Alexa Fluor 594 donkey anti-mouse secondary antibodies (Life Technologies, Inc.) for 2 h, and then the nuclei were stained with DAPI (Sigma) for 10 min. Finally, the cells were observed with an inverted system microscope Ti2-E (Nikon, Japan).

siRNA knockdown

siRNAs against the following mouse genes were synthesized with the following sequences, respectively: *Ahi1* 1, 5′-GCCACCUCAAUAUCAUUUATT-3′ and 5′-UAAAUGAUAUUGAGGUGGCTT-3′; *Ahi1* 2, 5′-GAUUUCUCACCCAAUGGUAAATT and 5′-UUUACCAUUGGGUGAGAAAUCTT-3′; *Rev-Erb*α, 5′-GCAUCGUUGUUCAACGUGATT-3′ and 5′-UCACGUUGAACAACGAUGCAA-3′; *Bmal1*, 5′-CAGUAAAGGUGGAAGAUAATT-3′ and 5′-UUAUCUUCCACCUUUACUGTT-3′. Cells were transfected with siRNAs using the Lipofectamine RNAiMAX transfection reagent (Invitrogen) according to the manufacturer's instructions.

Luciferase reporter assay

HEK293 cells were cotransfected with luciferase reporter and expression plasmids along with *Renilla* luciferase vector pRL-CMV as an internal control for normalization. The total amount of plasmid DNA was held constantly by the addition of empty plasmid. Cell extracts were prepared with Passive Lysis Buffer (Promega) 48 h after transfection, and the luciferase activities were measured with a Dual-Luciferase assay kit (Promega) using a microplate reader, Infinite M1000 Pro (Tecan), according to the manufacturer's instructions.

Immunoprecipitation assay

Cells were lysed in cell lysis buffer (50 mM Tris-HCl, pH 7.5, buffer containing 150 mM NaCl, 1% Nonidet P-40, and 0.5% deoxycholate) supplemented with the protease inhibitor mixture (Roche Applied Science) at 4 °C. After centrifugation at 12,000 $\times$ *g* for 15 min, the supernatants were used for immunoprecipitation with appropriate antibodies coupled to protein G-Sepharose beads (Roche Applied Science). The immunoprecipitants were then washed with cell lysis buffer and subjected to immunoblot analysis. The input represents 10% of the supernatant used in the co-immunoprecipitation experiments.

Immunoblot analysis

Cell extracts and midbrain tissue homogenates were lysed in cell lysis buffer. About 20 μg of proteins were electrophoresed and electrotransferred to a polyvinylidene difluoride membrane (Millipore). Blots were incubated with the following primary antibodies: polyclonal anti-AHI1 antibodies that were described previously (38), rabbit polyclonal anti-TH (AB152, Millipore), anti-NURR1 (sc-991, Santa Cruz Biotechnology, Inc.), anti-HA (sc-805, Santa Cruz Biotechnology), and anti-histone H2B (ab45695, Abcam) antibodies; rabbit monoclonal anti-TPH1 (ab52924, Abcam), anti-DDC (ab131282, Abcam), anti-MAOA (ab126751, Abcam), and anti-MAOB (ab125010, Abcam) antibodies; and mouse monoclonal anti-GFP (sc-9996, Santa Cruz Biotechnology), anti-FLAG (F3165, Sigma), anti-GAPDH (MAB374, Millipore), anti-CLOCK (sc-271603, Santa Cruz Biotechnology), anti-Rev-Erbα (sc-100910, Santa Cruz Biotechnology), and anti-BMAL1 (sc-365645, Santa Cruz Biotechnology) antibodies. The following secondary antibodies were used: horseradish peroxidase–conjugated sheep anti-mouse and anti-rabbit antibodies (Amersham Biosciences). The proteins were visualized with an ECL detection kit (Thermo) using a chemiluminescence imaging system (Bioshine ChemiQ 4800).

Real-time quantitative PCR (qPCR)

Total RNA was extracted from cells or midbrain tissues using TRIzol reagent (Invitrogen). Five hundred ng of each RNA sample was reverse-transcribed into cDNA for PCR assays with a PrimeScript RT Master Mix (Takara). Real-time PCR analysis

was performed for quantitative measurement of the target RNA abundance with power SYBR Green PCR Master Mix (Applied Biosystems) using a 7500 real-time PCR system (Applied Biosystems). Mouse primer sequences used for real-time PCR were as follows: 5′-GACAGGAGAACAAGTGGCAATG-3′ and 5′-ATCAGTGGTCAGCACGAACGA-3′ for *Ahi1*; 5′-GACCATCTTCCGAGAGCTAA-3′ and 5′-GGATGTTGTCTTCCCGATAG-3′ for *Tph1*; 5′-GTGGCTACAGGGAAGACAAC-3′ and 5′-AAGTCTCTTGGGCTCAGGTA-3′ for *Tph2*; 5′-GGTATACGCCACGCTGAAGG-3′ and 5′-TAGCCACAGTACCGTTCCAGA-3′ for *TH*; 5′-AAGAGCTGGGTTAATTGGTG-3′ and 5′-CAGTGTAGCGACCACAAAGA-3′ for *Ddc*; 5′-GCTGCTGTCTCATTGGGTCTC-3′ and 5′-CGAACTCAAACCAACCAATAGCC-3′ for *Comt*; 5′-GAGGCTCCAATTTCAATCACTCTG-3′ and 5′-ATGTAGTTTAGCAAGTCGTTCAGC-3′ for *Maoa*; 5′-AAGCGATGTGATCGTGGTGG-3′ and 5′-ACACTGAGGCCACAATCATGC-3′ for *Maob*; 5′-CTTCTCCTCTGGCTTCGTTGT-3′ and 5′-CAGGGTAGATGATGAAGATCAACC-3′ for *Dat*; 5′-GCGAGCATCTCTTATCTCATTGG-3′ and 5′-AAATGCTGATCCCAACAACTATC-3′ for *Vmat2*; 5′-ATCACGCTGGGTTTGGATAG-3′ and 5′-ATCACGCTGGGTTTGGATAG-3′ for *5-htt*; 5′-AGGGCACAAGCAACATTACC-3′ and 5′-CACAGGCGTGCACTCCATAG-3′ for *Rev-Erbα*; 5′-TGAAGAGAGCGGACAAGGAGATC-3′ and 5′-TCTGGAGTTAAGAAATCGGAGCTG-3′ for *Nurr1*; 5′-CAAGCACCTTCCTTCCAATG-3′ and 5′-GATTGCAGTCCACACCACTG-3′ for *Bmal1*; and 5′-GCTACAGCTTCACCACCACA-3′ and 5′-TCTCCAGGGAGGAAGAGGAT-3′ for *β-actin* as an internal control. Relative gene expression was calculated by the $2^{-\Delta\Delta CT}$ method.

Statistical analysis

Densitometric analysis of immunoblots from three independent experiments was calculated using Photoshop version 7.0 software (Adobe). The data were analyzed using Origin version 6.0 software (Originlab). Statistical analysis was performed by one-way analysis of variance (ANOVA). Student's *t* tests were used for comparing two groups. A p value of < 0.05 was considered statistically significant. All results are presented as means ± S.E.

Author contributions—D. G. data curation; D. G., H. S., and Z. H. software; D. G., Xingyun Xu, and Z. H. formal analysis; D. G., S. Z., and Xingyun Xu methodology; D. G. and H. R. writing-original draft; S. Z. validation; S. Z., H. S., and C. M. investigation; C. M., G. W., and H. R. supervision; C. M. project administration; Xingshun Xu resources; G. W. and H. R. conceptualization; G. W. and H. R. funding acquisition; G. W. and H. R. writing-review and editing.

Acknowledgments—We thank Dr. Ying Xu (CAM-SU Genomic Resource Center at Soochow University) for providing HA-CLOCK, HA-BMAL1, FLAG-RORα, wildtype mouse Bmal1-luciferase, and mutant Bmal1-luciferase plasmids. We thank Dr. Joseph Gleeson for providing the pEGFP-C3-AHI1 plasmid.

References

1. Ferland, R. J., Eyaid, W., Collura, R. V., Tully, L. D., Hill, R. S., Al-Nouri, D., Al-Rumayyan, A., Topcu, M., Gascon, G., Bodell, A., Shugart, Y. Y., Ruvolo, M., and Walsh, C. A. (2004) Abnormal cerebellar development and axonal decussation due to mutations in AHI1 in Joubert syndrome. *Nat. Genet.* **36,** 1008–1013 CrossRef Medline
2. Utsch, B., Sayer, J. A., Attanasio, M., Pereira, R. R., Eccles, M., Hennies, H. C., Otto, E. A., and Hildebrandt, F. (2006) Identification of the first AHI1 gene mutations in nephronophthisis-associated Joubert syndrome. *Pediatr. Nephrol.* **21,** 32–35 CrossRef Medline
3. Valente, E. M., Brancati, F., Silhavy, J. L., Castori, M., Marsh, S. E., Barrano, G., Bertini, E., Boltshauser, E., Zaki, M. S., Abdel-Aleem, A., Abdel-Salam, G. M., Bellacchio, E., Battini, R., Cruse, R. P., Dobyns, W. B., *et al.* (2006) AHI1 gene mutations cause specific forms of Joubert syndrome-related disorders. *Ann. Neurol.* **59,** 527–534 CrossRef Medline
4. Amann-Zalcenstein, D., Avidan, N., Kanyas, K., Ebstein, R. P., Kohn, Y., Hamdan, A., Ben-Asher, E., Karni, O., Mujaheed, M., Segman, R. H., Maier, W., Macciardi, F., Beckmann, J. S., Lancet, D., and Lerer, B. (2006) AHI1, a pivotal neurodevelopmental gene, and C6orf217 are associated with susceptibility to schizophrenia. *Eur. J. Hum. Genet.* **14,** 1111–1119 CrossRef Medline
5. Ingason, A., Giegling, I., Cichon, S., Hansen, T., Rasmussen, H. B., Nielsen, J., Jürgens, G., Muglia, P., Hartmann, A. M., Strengman, E., Vasilescu, C., Mühleisen, T. W., Djurovic, S., Melle, I., Lerer, B., *et al.* (2010) A large replication study and meta-analysis in European samples provides further support for association of AHI1 markers with schizophrenia. *Hum. Mol. Genet.* **19,** 1379–1386 CrossRef Medline
6. Ingason, A., Sigmundsson, T., Steinberg, S., Sigurdsson, E., Haraldsson, M., Magnusdottir, B. B., Frigge, M. L., Kong, A., Gulcher, J., Thorsteinsdottir, U., Stefansson, K., Petursson, H., and Stefansson, H. (2007) Support for involvement of the AHI1 locus in schizophrenia. *Eur. J. Hum. Genet.* **15,** 988–991 CrossRef Medline
7. Rivero, O., Reif, A., Sanjuán, J., Moltó, M. D., Kittel-Schneider, S., Nájera, C., Töpner, T., and Lesch, K. P. (2010) Impact of the AHI1 gene on the vulnerability to schizophrenia: a case-control association study. *PLoS One* **5,** e12254 CrossRef Medline
8. Porcelli, S., Pae, C. U., Han, C., Lee, S. J., Patkar, A. A., Masand, P. S., Balzarro, B., Alberti, S., De Ronchi, D., and Serretti, A. (2014) Abelson helper integration site-1 gene variants on major depressive disorder and bipolar disorder. *Psychiatry Investig.* **11,** 481–486 CrossRef Medline
9. Alvarez Retuerto, A. I., Cantor, R. M., Gleeson, J. G., Ustaszewska, A., Schackwitz, W. S., Pennacchio, L. A., and Geschwind, D. H. (2008) Association of common variants in the Joubert syndrome gene (AHI1) with autism. *Hum. Mol. Genet.* **17,** 3887–3896 CrossRef Medline
10. Ren, L., Qian, X., Zhai, L., Sun, M., Miao, Z., Li, J., and Xu, X. (2014) Loss of Ahi1 impairs neurotransmitter release and causes depressive behaviors in mice. *PLoS One* **9,** e93640 CrossRef Medline
11. Xu, X., Yang, H., Lin, Y. F., Li, X., Cape, A., Ressler, K. J., Li, S., and Li, X. J. (2010) Neuronal Abelson helper integration site-1 (Ahi1) deficiency in mice alters TrkB signaling with a depressive phenotype. *Proc. Natl. Acad. Sci. U.S.A.* **107,** 19126–19131 CrossRef Medline
12. Weng, L., Lin, Y. F., Li, A. L., Wang, C. E., Yan, S., Sun, M., Gaertig, M. A., Mitha, N., Kosaka, J., Wakabayashi, T., Xu, X., Tang, B., Li, S., and Li, X. J. (2013) Loss of Ahi1 affects early development by impairing BM88/Cend1-mediated neuronal differentiation. *J. Neurosci.* **33,** 8172–8184 CrossRef Medline
13. Blier, P. (2013) Neurotransmitter targeting in the treatment of depression. *J. Clin. Psychiatry* **74,** 19–24 CrossRef Medline
14. Meyer, J. H. (2008) Applying neuroimaging ligands to study major depressive disorder. *Semin. Nucl. Med.* **38,** 287–304 CrossRef Medline
15. Southwick, S. M., Vythilingam, M., and Charney, D. S. (2005) The psychobiology of depression and resilience to stress: implications for prevention and treatment. *Annu. Rev. Clin. Psychol.* **1,** 255–291 CrossRef Medline
16. Charney, D. S. (2004) Psychobiological mechanisms of resilience and vulnerability: implications for successful adaptation to extreme stress. *Am. J. Psychiatry* **161,** 195–216 CrossRef Medline
17. Dunlop, B. W., and Nemeroff, C. B. (2007) The role of dopamine in the pathophysiology of depression. *Arch. Gen. Psychiatry* **64,** 327–337 CrossRef Medline
18. Ashok, A. H., Marques, T. R., Jauhar, S., Nour, M. M., Goodwin, G. M., Young, A. H., and Howes, O. D. (2017) The dopamine hypothesis of bipo-

lar affective disorder: the state of the art and implications for treatment. *Mol. Psychiatry* **22,** 666–679 CrossRef Medline
19. Bellivier, F., Geoffroy, P. A., Etain, B., and Scott, J. (2015) Sleep- and circadian rhythm-associated pathways as therapeutic targets in bipolar disorder. *Expert Opin. Ther. Targets* **19,** 747–763 CrossRef Medline
20. Albrecht, U. (2017) Molecular Mechanisms in mood regulation involving the circadian clock. *Front. Neurol.* **8,** 30 Medline
21. Bunney, B. G., Li, J. Z., Walsh, D. M., Stein, R., Vawter, M. P., Cartagena, P., Barchas, J. D., Schatzberg, A. F., Myers, R. M., Watson, S. J., Akil, H., and Bunney, W. E. (2015) Circadian dysregulation of clock genes: clues to rapid treatments in major depressive disorder. *Mol. Psychiatry* **20,** 48–55 CrossRef Medline
22. Korshunov, K. S., Blakemore, L. J., and Trombley, P. Q. (2017) Dopamine: a modulator of circadian rhythms in the central nervous system. *Front. Cell Neurosci.* **11,** 91 Medline
23. Chung, S., Lee, E. J., Yun, S., Choe, H. K., Park, S. B., Son, H. J., Kim, K. S., Dluzen, D. E., Lee, I., Hwang, O., Son, G. H., and Kim, K. (2014) Impact of circadian nuclear receptor REV-ERBα on midbrain dopamine production and mood regulation. *Cell* **157,** 858–868 CrossRef Medline
24. Jager, J., O'Brien, W. T., Manlove, J., Krizman, E. N., Fang, B., Gerhart-Hines, Z., Robinson, M. B., Klein, P. S., and Lazar, M. A. (2014) Behavioral changes and dopaminergic dysregulation in mice lacking the nuclear receptor Rev-erbα. *Mol. Endocrinol.* **28,** 490–498 CrossRef Medline
25. Zetterström, R. H., Solomin, L., Jansson, L., Hoffer, B. J., Olson, L., and Perlmann, T. (1997) Dopamine neuron agenesis in Nurr1-deficient mice. *Science* **276,** 248–250 CrossRef Medline
26. McClung, C. A., Sidiropoulou, K., Vitaterna, M., Takahashi, J. S., White, F. J., Cooper, D. C., and Nestler, E. J. (2005) Regulation of dopaminergic transmission and cocaine reward by the Clock gene. *Proc. Natl. Acad. Sci. U.S.A.* **102,** 9377–9381 CrossRef Medline
27. Sidor, M. M., Spencer, S. M., Dzirasa, K., Parekh, P. K., Tye, K. M., Warden, M. R., Arey, R. N., Enwright, J. F., 3rd, Jacobsen, J. P., Kumar, S., Remillard, E. M., Caron, M. G., Deisseroth, K., and McClung, C. A. (2015) Daytime spikes in dopaminergic activity drive rapid mood-cycling in mice. *Mol. Psychiatry* **20,** 1406–1419 CrossRef Medline
28. Roybal, K., Theobold, D., Graham, A., DiNieri, J. A., Russo, S. J., Krishnan, V., Chakravarty, S., Peevey, J., Oehrlein, N., Birnbaum, S., Vitaterna, M. H., Orsulak, P., Takahashi, J. S., Nestler, E. J., Carlezon, W. A., Jr., and McClung, C. A. (2007) Mania-like behavior induced by disruption of CLOCK. *Proc. Natl. Acad. Sci. U.S.A.* **104,** 6406–6411 CrossRef Medline
29. Hampp, G., Ripperger, J. A., Houben, T., Schmutz, I., Blex, C., Perreau-Lenz, S., Brunk, I., Spanagel, R., Ahnert-Hilger, G., Meijer, J. H., and Albrecht, U. (2008) Regulation of monoamine oxidase A by circadian-clock components implies clock influence on mood. *Curr. Biol.* **18,** 678–683 CrossRef Medline
30. Lemos, D. R., Goodspeed, L., Tonelli, L., Antoch, M. P., Ojeda, S. R., and Urbanski, H. F. (2007) Evidence for circadian regulation of activating transcription factor 5 but not tyrosine hydroxylase by the chromaffin cell clock. *Endocrinology* **148,** 5811–5821 CrossRef Medline
31. Triqueneaux, G., Thenot, S., Kakizawa, T., Antoch, M. P., Safi, R., Takahashi, J. S., Delaunay, F., and Laudet, V. (2004) The orphan receptor Rev-erbalpha gene is a target of the circadian clock pacemaker. *J. Mol. Endocrinol.* **33,** 585–608 CrossRef Medline
32. Preitner, N., Damiola, F., Lopez-Molina, L., Zakany, J., Duboule, D., Albrecht, U., and Schibler, U. (2002) The orphan nuclear receptor REV-ERBalpha controls circadian transcription within the positive limb of the mammalian circadian oscillator. *Cell* **110,** 251–260 CrossRef Medline
33. Partch, C. L., Green, C. B., and Takahashi, J. S. (2014) Molecular architecture of the mammalian circadian clock. *Trends Cell Biol.* **24,** 90–99 CrossRef Medline
34. Akashi, M., and Takumi, T. (2005) The orphan nuclear receptor RORα regulates circadian transcription of the mammalian core-clock Bmal1. *Nat. Struct. Mol. Biol.* **12,** 441–448 CrossRef Medline
35. Tekin, I., Roskoski, R., Jr, Carkaci-Salli, N., and Vrana, K. E. (2014) Complex molecular regulation of tyrosine hydroxylase. *J. Neural Transm.* **121,** 1451–1481 CrossRef Medline
36. Furlong, R. A., Rubinsztein, J. S., Ho, L., Walsh, C., Coleman, T. A., Muir, W. J., Paykel, E. S., Blackwood, D. H., and Rubinsztein, D. C. (1999) Analysis and metaanalysis of two polymorphisms within the tyrosine hydroxylase gene in bipolar and unipolar affective disorders. *Am. J. Med. Genet.* **88,** 88–94 CrossRef Medline
37. Serretti, A., Macciardi, F., Verga, M., Cusin, C., Pedrini, S., and Smeraldi, E. (1998) Tyrosine hydroxylase gene associated with depressive symptomatology in mood disorder. *Am. J. Med. Genet.* **81,** 127–130 CrossRef Medline
38. Sheng, G., Xu, X., Lin, Y. F., Wang, C. E., Rong, J., Cheng, D., Peng, J., Jiang, X., Li, S. H., and Li, X. J. (2008) Huntingtin-associated protein 1 interacts with Ahi1 to regulate cerebellar and brainstem development in mice. *J. Clin. Invest.* **118,** 2785–2795 CrossRef Medline
39. Fukuchi, M., Fujii, H., Takachi, H., Ichinose, H., Kuwana, Y., Tabuchi, A., and Tsuda, M. (2010) Activation of tyrosine hydroxylase (TH) gene transcription induced by brain-derived neurotrophic factor (BDNF) and its selective inhibition through Ca^{2+} signals evoked via the *N*-methyl-D-aspartate (NMDA) receptor. *Brain Res.* **1366,** 18–26 CrossRef Medline
40. Jang, S. W., Liu, X., Pradoldej, S., Tosini, G., Chang, Q., Iuvone, P. M., and Ye, K. (2010) *N*-Acetylserotonin activates TrkB receptor in a circadian rhythm. *Proc. Natl. Acad. Sci. U.S.A.* **107,** 3876–3881 CrossRef Medline
41. Karatsoreos, I. N. (2014) Links between circadian rhythms and psychiatric disease. *Front. Behav. Neurosci.* **8,** 162 Medline
42. McCarthy, M. J., and Welsh, D. K. (2012) Cellular circadian clocks in mood disorders. *J. Biol. Rhythms* **27,** 339–352 CrossRef Medline
43. Lamont, E. W., Legault-Coutu, D., Cermakian, N., and Boivin, D. B. (2007) The role of circadian clock genes in mental disorders. *Dialogues Clin. Neurosci.* **9,** 333–342 Medline
44. Dallaspezia, S., and Benedetti, F. (2015) Chronobiology of bipolar disorder: therapeutic implication. *Curr. Psychiatry Rep.* **17,** 606 Medline
45. Lamont, E. W., Coutu, D. L., Cermakian, N., and Boivin, D. B. (2010) Circadian rhythms and clock genes in psychotic disorders. *Isr. J. Psychiatry Relat. Sci.* **47,** 27–35 Medline
46. Wulff, K., Gatti, S., Wettstein, J. G., and Foster, R. G. (2010) Sleep and circadian rhythm disruption in psychiatric and neurodegenerative disease. *Nat. Rev. Neurosci.* **11,** 589–599 CrossRef Medline
47. Barandas, R., Landgraf, D., McCarthy, M. J., and Welsh, D. K. (2015) Circadian clocks as modulators of metabolic comorbidity in psychiatric disorders. *Curr. Psychiatry Rep.* **17,** 98 CrossRef Medline
48. De Bundel, D., Gangarossa, G., Biever, A., Bonnefont, X., and Valjent, E. (2013) Cognitive dysfunction, elevated anxiety, and reduced cocaine response in circadian clock-deficient cryptochrome knockout mice. *Front. Behav. Neurosci.* **7,** 152 Medline
49. Kondratova, A. A., Dubrovsky, Y. V., Antoch, M. P., and Kondratov, R. V. (2010) Circadian clock proteins control adaptation to novel environment and memory formation. *Aging* **2,** 285–297 CrossRef Medline
50. Lancaster, M. A., Louie, C. M., Silhavy, J. L., Sintasath, L., Decambre, M., Nigam, S. K., Willert, K., and Gleeson, J. G. (2009) Impaired Wnt-β-catenin signaling disrupts adult renal homeostasis and leads to cystic kidney ciliopathy. *Nat. Med.* **15,** 1046–1054 CrossRef Medline
51. Gu, C., Zhang, Y., Hu, Q., Wu, J., Ren, H., Liu, C. F., and Wang, G. (2017) P7C3 inhibits GSK3β activation to protect dopaminergic neurons against neurotoxin-induced cell death *in vitro* and *in vivo*. *Cell Death Dis.* **8,** e2858 CrossRef Medline
52. Gundersen, H. J., Bagger, P., Bendtsen, T. F., Evans, S. M., Korbo, L., Marcussen, N., Møller, A., Nielsen, K., Nyengaard, J. R., and Pakkenberg, B. (1988) The new stereological tools: disector, fractionator, nucleator and point sampled intercepts and their use in pathological research and diagnosis. *APMIS* **96,** 857–881 CrossRef Medline